# Mode-locked laser driven gates for trapped ion quantum information processing

Wesle y C. Campbell  Charles Conover*  David Hayes
David Hucul  Dzmitry N. Matsukevich  Peter Maunz
Jonathan Mizrahi  Steven Olmschenk  Qudsia Quraishi
Crystal Senko  Chris Monroe

Joint Quantum Institute, University of Maryland Department of Physics and National Institute of Standards and Technology, College Park, MD 20742 USA

**Abstract** Single- and multi-qubit operations for trapped ion hyperfine or Zeeman qubits are typically implemented by continuous-wave lasers driving stimulated Raman transitions. Here we report two distinct regimes for driving these transitions with mode-locked pulsed lasers instead of cw systems. In the resolved-sideband regime, multiple pulses from a mode-locked laser constructively accumulate transition amplitude to drive the gate. In the regime where the pulse train is shorter than the oscillation period of motional modes, the mode spectrum is unresolvable and all allowed sidebands are driven simultaneously. We demonstrate a single qubit gate in about 50 ps in this regime, and discuss extensions to multi-qubit gates.

PACS: 03.67.Lx, 03.67.Bg, 32.80.Qk, 37.10.Rs, 37.10.Vz, 37.25.+k
Keywords: Trapped ion, Mode-locked laser, Stimulated Raman transition, Quantum gate

## 1 Introduction

We demonstrate the use of a mode-locked laser to drive trapped ion qubit quantum gates as a replacement for continuous-wave (cw) lasers [1]. The efficient use of these high-power lasers allows operation far from resonance, suppressing laser-induced decoherence. We also extend this work into faster laser-atom interactions where the motional sidebands are no longer resolved [2].

## 2 Resolved-sideband regime operations

### *2.1 Frequency combs for stimulated Raman transitions*

In most trapped ion hyperfine qubit quantum information processors, cw stimulated Raman transitions are driven by simultaneously applying two beams to the ion with a beatnote whose frequency matches the atomic transition frequency. This process may also be implemented via

* Colby College Department of Physics and Astronomy, Waterville, ME 04901 USA

mode-locked lasers in a way that they may essentially be thought of as an ensemble of cw lasers with just the right beatnotes between them.

Fig. 1 shows a schematic of the principle behind this type of stimulated Raman transition. In the time domain, if a single pulse is sufficiently weak as to have an almost negligible effect on state of the atomic qubit, it is clear that in order to drive a transition we require many pulses to be applied. Furthermore, we require that the desired transition amplitude from pulse to pulse constructively interfere in order to make this process efficient. In this case, the target amplitude coherently accumulates over the duration of the pulse train while all other amplitudes do not. This is accomplished by controlling the arrival time of the pulses (generally fixed by the repetition rate of the laser, $f_{\text{rep}}$). For a pure atomic state transition (carrier transition), the Bloch vector must make an integer number of orbits around the Bloch sphere during the free-evolution period between pulses so that the next pulse arrives at just the right time to rotate the state vector about the same axis as the previous pulse.

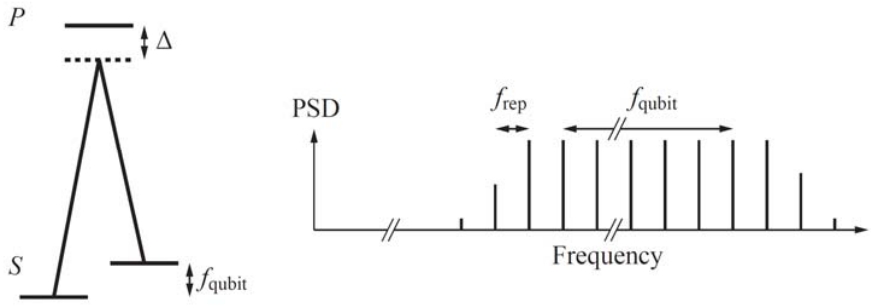


**Figure 1:** Frequency domain representation of stimulated Raman transitions from an optical frequency comb.

This can also be understood in the frequency domain. For the special case where the carrierenvelope phase change from pulse to pulse (CEP) is stable, the pulse train is an optical frequency comb. If the teeth of this comb are spaced by the right amount, there will be pairs of teeth that make the appropriate beatnote between them to drive the transition. For both the time-domain and frequency-domain pictures, we find that the condition for driving a transition between two states split by $f_{\text{qubit}}$ is simply expressed by

$$\frac{f_{\text{qubit}}}{f_{\text{rep}}} \in \mathbb{Z}. \tag{1}$$

To drive motional sideband transitions, the pulse train is split into two on a beamsplitter and directed onto the ion from different directions to increase the Lamb-Dicke factor. In this case, Condition (1) should be violated on purpose by adjusting the laser rep rate to ensure a single beam cannot drive carrier transitions during the motional sideband transition. The coherent accumulation can be restored, however, by frequency shifting one of the two beams with, for instance, an acousto-optic modulator. The magnitude of the appropriate shift is found by guaranteeing that the transition frequency is equal to the beatnote between two comb teeth, each necessarily from separate combs. The condition for driving a motional transition in this configuration is given by

$$\frac{f_{\text{qubit}} + f_{\text{AOM}}}{f_{\text{rep}}} \in \mathbb{Z} \tag{2}$$

where $f_{AOM}$ is the magnitude of the frequency shift created between the two beams (this would be the beatnote for cw lasers).

Using these techniques, we have demonstrated the full range of Raman transition tasks for which we previously used cw lasers [1]. This includes single-qubit operations, motional sideband transitions, spin-motion entanglement, and entanglement of the internal states of multiple ions. Mode-locked lasers can therefore be used as a replacement for cw lasers in such systems, and offer distinct advantages, as discussed below. Furthermore, it is worth noting explicitly that CEP stability is unnecessary for Raman transitions. Even if the carrier-envelope phase is completely randomized from pulse to pulse, which does not create an optical frequency comb, the microwave comb created by the pulse envelopes remains intact and the transition is still driven with no loss of efficiency.

### *2.2 Large detuning and optimal wavelength for low decoherence*

The primary advantage of using mode-locked lasers instead of cw lasers for stimulated Raman transitions is the available power. Most ions favored for trapped ion quantum information have transitions in the UV, where high laser power is difficult to obtain. Furthermore, the creation of two cw beams that are phase-locked with a multi-GHz beatnote between them is inefficient with an EOM and costly with two separate lasers, further reducing the available power. As a result, the detuning of the cw beams from resonance with the S ↔ P transition (Δ, see Fig. 1) is typically reduced to enhance the Raman transition Rabi frequency. The proximity of this laser frequency to a dipole-allowed transition therefore tends to cause decoherence during the gate.

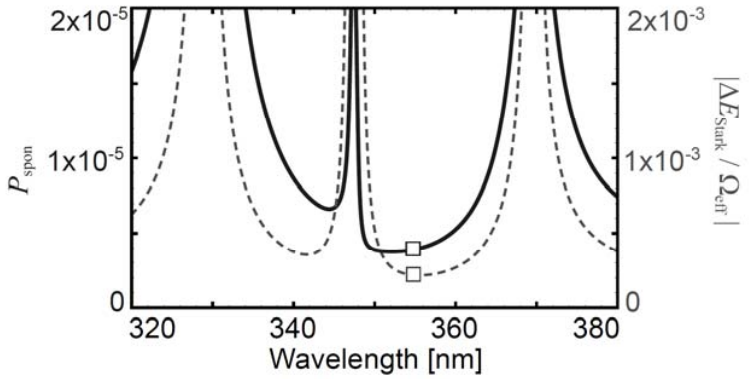


**Figure 2:** The probability of a spontaneous emission event during a stimulated Raman π-pulse (solid line, left axis) and differential AC Stark shift divided by Raman transition Rabi frequency (dashed line, right axis) vs. laser wavelength for $^{171}Yb^{+}$. The squares indicate the wavelength of a frequency-tripled vanadate laser.

The two main mechanisms for this laser-induced decoherence are spontaneous emission from the excited state (rat $\Gamma_{spon}$) and differential energy shifts ($\Delta E_{Stark}$) of the qubit states due to the intensity of the laser ($I$) via the AC Stark effect. The rates of these decoherence mechanisms are proportional to $I/\Delta^2$, indicating that larger detuning is desirable. However, the Raman transition Rabi frequency also falls off with increasing detuning ($\Omega_{eff} \propto I/\Delta$), so Δ cannot be increased with impunity. Furthermore, slowing the gate down by increasing Δ also increases the bandwidth of laser noise that can decohere the qubit. Figure 2 shows the spontaneous emission probability during an stimulated Raman π-pulse as a function of wavelength for $^{171}Yb^{+}$. There is a clear minimum near 355 nm, which can be viewed as a sort of optimum

wavelength for this system. However, this represents a tremendously large detuning $\Delta \sim 33$ THz and Watts of power are needed to operate there with reasonably high $\Omega_{\text{eff}}$.

The mode-locked laser addresses these issues by providing more power with the desired frequency content, permitting operation at significantly larger detuning ($\Delta$). The UV wavelengths needed become much easier and more efficient to generate with pulsed lasers than cw due to the nonlinear nature of the harmonic generation efficiency. It is the instantaneous intensity of the light that determines the harmonic output in these nonlinear crystals, so for the same average power, the mode-locked laser will be far more efficiently converted to higher harmonics. Also, the multi-GHz beatnote itself is built into the pulse due to its bandwidth, so a highly efficient, low frequency device such as an AOM can be used to create a high frequency beatnote via Condition (2).

# 3 Fast gates

The dramatic reduction in laser-induced decoherence that can be expected from replacing cw lasers with a high power mode-locked laser offer advantages for operations requiring spectroscopic resolution of motional sidebands. However, as the gate time is decreased below the motional period of the ions, these spectral features become unresolvable and new types of gates are needed to utilize these fast operations. Fig. 3 shows the spectrum of a single, trapped ion taken with a 355 nm mode-locked laser for varying pulse train durations. Despite being more than 10 nm away from the nearest strong transition, there is sufficient optical power available in these lasers to push the gate time well below 1 μs. In this regime, the sidebands are no longer resolved since the comb teeth become wider than the mode spacing (see Fig. 3).

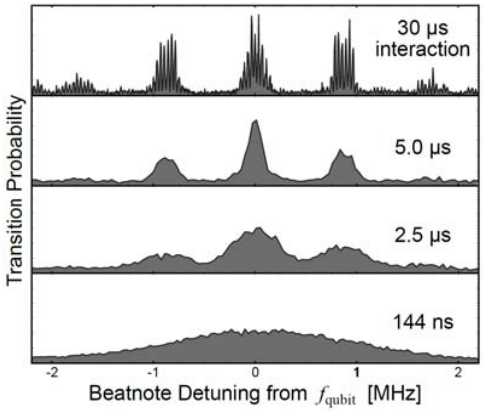


**Figure 3:** Stimulated Raman transition spectra of a single trapped $^{171}Yb^{+}$ ion taken with a modelocked 355 nm laser for various pulse train durations. As the pulse train duration decreases, the motional sidebands become unresolved from one another.

### *3.1 Single-qubit operations*

For single-qubit operations, a single laser beam illuminating the ion from one direction is sufficient to drive transitions. If the pulse bandwidth is larger than the qubit splitting ($1/T_{\text{pulse}} >> f_{\text{qubit}}$), even a single pulse has all of the necessary frequency content to drive a stimulated Raman transition. The pulse shape, however, can still limit the maximum transition probability from a single pulse [3]. To overcome this limitation, we split the pulse into two and added a variable delay between the two halves of the pulse to achieve a ful π-pulse in about

50 ps [2]. To first order, the appropriate delay is given by Condition (1). This represents a dramatic speed up in gate time, and as a fraction of the qubit storage coherence time this gate duration is negligibly small.

### *3.2 Beyond resolved sidebands*

The bottom frame of Fig. 3 shows a Raman spectrum for a gate time much less than the motional period of the ion. These data were taken with counterpropagating combs with a relative shift of $f_{\mathrm{AOM}}$ between them. In this regime, all of the sidebands are driven simultaneously. The interaction Hamiltonian is given by

$$\hat{H} = -\frac{\Omega_{\mathrm{eff}}}{2}\left( \mathrm{e}^{\mathrm{i}\eta\left(\hat{a}^{\dagger}+\hat{a}\right)+\mathrm{i}\phi(t)} + \mathrm{e}^{-\mathrm{i}\eta\left(\hat{a}^{\dagger}+\hat{a}\right)-\mathrm{i}\phi(t)} \right)\hat{\sigma}_{x} \tag{3}$$

where $\Omega_{\mathrm{eff}}(t)$ is the pulse envelope, $\eta$ is the Lamb-Dicke factor, $\hat{a}$ and $\hat{a}^{\dagger}$ are the motional mode phonon annihilation and creation operators, and $\phi(t) = 2\pi f_{\mathrm{AOM}} t$ is the shift caused by the acousto-optic modulator. We can define the integrated pulse area $\theta \equiv \int \mathrm{d}t\,\Omega_{\mathrm{eff}}(t)$ to write the time-evolution operator in the limit where the pulse duration is short compared to both the internal and motional state evolution:

$$\begin{aligned} \hat{U} &= \mathrm{e}^{\mathrm{i}\theta\cos\left(\eta\left(\hat{a}^{\dagger}+\hat{a}\right)+\phi(t_0)\right)\hat{\sigma}_{x}} \\ &= \sum_{n=-\infty}^{\infty} (\mathrm{i})^{n}\,\mathrm{e}^{\mathrm{i}\phi(t_0)} J_{n}(\theta)\,\hat{D}[i\eta n]\hat{\sigma}_{x}^{n} \end{aligned} \tag{4}$$

Here, $t_0$ is the time when the pulse arrives and $\hat{D}[\alpha]$ is the displacement operator for coherent states of the phonon harmonic oscillator.

Equation (4) illustrates the diffractive effect of the standing wave created by the pulses when they overlap on the ion. The initial state is split into a series of diffracted orders, each displaced by integer multiples of $\eta$ in momentum space. The $n^{\mathrm{th}}$ diffracted order has an amplitude proportional to the Bessel function $J_n$, as expected for Raman-Nath diffraction.

Entangling gates that operate faster than the motional periods of ions in the trap have been proposed in Ref. [4, 5]. These gates should scale favorably to large numbers of ions and are predicted to be insensitive to temperature. Both types are built from a series of spin-dependent momentum kicks, where the direction of the kick depends on the internal qubit state of the atom. Eq. (4), however, shows that a single kick will diffract the atoms into a large number of momentum states, so we once again need to rely on coherent accumulation from a pulse train to create a spin-dependent momentum kick. We anticipate that a short pulse train (~ 10 pulses) can be used to create such a kick, whereby the transition amplitude to the appropriate diffracted orders interferes constructively and all other orders do not. In the limit where the pulse train duration is short enough that the trap motion can be ignored between pulses, the condition for creating a spin-dependent kick converges to Condition (2). By applying a series of these kicks, we hope to implement these new, scalable gates for trapped atomic ions.

# References


[1] D. Hayes, D. N. Matsukevich, P. Maunz, D. Hucul, Q. Quraishi, S. Olmschenk, W. Campbell, J. Mizrahi, C. Senko, and C. Monroe, Phys. Rev. Lett., **104**, 140501 (2010).

[2] W. C. Campbell, J. Mizrahi, Q. Quraishi, C. Senko, D. Hayes, D. Hucul, D. N. Matsukevich, P. Maunz, and C. Monroe, Phys. Rev. Lett., **105,** 090502 (2010).

[3] N. Rosen and C. Zener, Phys. Rev., **40,** 502 (1932).

[4] J. J. García-Ripoll, P. Zoller, and J. I. Cirac, Phys. Rev. Lett., **91,** 157901 (2003).
[5] L.-M. Duan, Phys. Rev. Lett., **93,** 100502 (2004).